ELSEVIER

Journal of Magnetism and Magnetic Materials 154 (1996) 29–36

Journal of magnetism and magnetic materials

The antiphase domain magnetic structure of the $DyGe_3$ compound

P. Schobinger-Papamantellos [a,*], T. Janssen [b], K.H.J. Buschow [c]

[a] *Laboratorium für Kristallographie ETH Zentrum CH-8092 Zürich, Switzerland*

[b] *Institute for Theoretical Physics, University of Nijmegen 6525 ED Nijmegen, The Netherlands*

[c] *Van der Waals–Zeeman Institute, University of Amsterdam, Valckeniersstraat 65, 1018 XE, Amsterdam, The Netherlands*

Received 17 July 1995

Abstract

The magnetic properties of the novel compound $DyGe_3$ have been studied by neutron diffraction and magnetic measurements. $DyGe_3$ (orthorhombic Cmcm, $Z = 4$) orders antiferromagnetically at $T_N = 24$ K. The superstructure lines observed in the neutron powder data require a sixfold cell enlargement of the primitive chemical cell upon magnetic ordering ($2\boldsymbol{a}$, $(\boldsymbol{a}+\boldsymbol{b})/2$, $3\boldsymbol{c}$) and a twofold splitting of the atomic positions. The magnetic space group is P_a2_1/m. The two Dy sublattices have a uniaxial moment arrangement along c and are coupled antiferromagnetically with the same ordered moment values $8.1\,\mu_B$ below 8 K. Their different temperature dependencies are discussed in terms of a Fourier analysis of the observed data over the whole magnetically ordered region.

1. Introduction

In a recent publication [1] we reported on the structure of a novel type binary Dy–Ge compound of composition $DyGe_3$ on the basis of X-ray and neutron powder diffraction data. This structure has been described as a stacking variable of the CrB-type structure of DyGe with a change of the stacking sequence along the $\boldsymbol{b}$-axis by introducing four Ge atomic layers perpendicular to it. The building blocks (which are also favoured by other rare earth germanium and silicon compounds) of the CrB structure are trigonal rare earth prisms centered by germanium or silicon which are stacked in a double-layer arrangement parallel to the (010) plane.

The structural similarity is also displayed by the lattice constants, $\boldsymbol{a}$ and $\boldsymbol{c}$ of the two compounds are comparable, while $\boldsymbol{b}$ of $DyGe_3$ is almost twice that of DyGe ($a = 0.4254(1)$ nm, $b = 1.0623(2)$ nm, $c = 0.3904(1)$ nm for DyGe and $a = 0.40278(5)$ nm, $b = 2.0710(3)$ nm, $c = 0.38997(5)$ nm for $DyGe_3$). Both compounds crystallize with the orthorhombic space group Cmcm (No. 63), $Z = 4$, and all atoms occupy the 4(c) Wyckoff position $(0, y, 1/4)$.

DyGe, like all heavy rare earth germanium and silicon compounds, orders antiferromagnetically below $T_N = 37$ K. Its uniaxial magnetic moment arrangement is associated with a cell doubling in the $\boldsymbol{c}$ direction [2]. The Dy moments are oriented along the $\boldsymbol{c}$ direction but have opposite directions when going from one cell to the other in the $\boldsymbol{c}$ direction. In view of the similarity between DyGe and $DyGe_3$ it is of interest to study the magnetic properties also of $DyGe_3$.

* Corresponding author. Fax: +41-1-632-1133; email: nelly@kristall.erdw.ethz.ch.

SSDI 0304-8853(95)00578-1

2. Experimental

Results of magnetic measurements made for $DyGe_3$ on a SQUID magnetometer are shown in Fig. 1. From these data it can be derived that $DyGe_3$ orders antiferromagnetically below $T_N = 24$ K. Also shown in Fig. 1 is a plot of the temperature dependence of the reciprocal susceptibility. From this plot one derives $\theta_p = -33$ K and $\mu_{eff} = 10.49\mu_B$/Dy, the latter value being close to the free-ion value ($10.63\mu_B$/Dy).

The neutron diffraction data (performed on the same sample and under the same experimental conditions in the reactor Saphir in Würenlingen, as described in Ref. [1]) were collected for various temperatures in the range 8–30 K ($\lambda = 1.7012$ Å).

3. Results and discussion

3.1. Magnetic ordering

In the magnetically ordered state as shown in Fig. 2, one observes a large number of additional peaks of magnetic origin in the low-angle 2θ region. These are situated at different reciprocal lattice positions than those of the nuclear cell, therefore $\boldsymbol{k} \neq 0$. Their indexing has been possible by assuming a sixfold cell enlargement of the monoclinic primitive nuclear cell $(2\boldsymbol{a}, (\boldsymbol{a}+\boldsymbol{b})/2, 3\boldsymbol{c})$ where $\boldsymbol{a}$, $\boldsymbol{b}$ and $\boldsymbol{c}$ refer to the orthorhombic C-centered lattice.

From the observed systematic extinctions ((hkl), $h = 2n$ and $0kl$ all absent for all k and l) one is led to an anticentered magnetic monoclinic lattice denoted P_a with the translations $(\boldsymbol{a}',\boldsymbol{b}',\boldsymbol{c}')$ and the antitranslation (1/2, 0, 0). This has a consequence that atoms related by the C-centering translation in the orthorhombic cell have their moments parallel, and all calculations have to refer to the reduced primitive cell with the symmetry $P112_1/m$ [3]. Taking into account the antitranslation operation (1/2, 0, 0), one can derive the magnetic space group P_a2_1/m (Sh_{11}^{56}) [4], provided that no further symmetry reduction occurs.

The relation between the P_a monoclinic cell and the orthorhombic C-cell is shown in Fig. 3. The transformations for various physical quantities from one axial system to the other are

$$(\boldsymbol{a}',\boldsymbol{b}',\boldsymbol{c}') = (\boldsymbol{a},\boldsymbol{b},\boldsymbol{c})\boldsymbol{P},$$

$$\begin{pmatrix} x' \\ y' \\ z' \end{pmatrix} = \boldsymbol{Q}\begin{pmatrix} x \\ y \\ z \end{pmatrix}, \quad \begin{pmatrix} \boldsymbol{a}'^* \\ \boldsymbol{b}'^* \\ \boldsymbol{c}'^* \end{pmatrix} = \boldsymbol{Q}\begin{pmatrix} \boldsymbol{a}^* \\ \boldsymbol{b}^* \\ \boldsymbol{c}^* \end{pmatrix}, \tag{1}$$

where the primed symbols refer to the monoclinic lattice and those without primes refer to the orthorhombic lattice:

$$\boldsymbol{P} = \begin{pmatrix} 2 & 1/2 & 0 \\ 0 & 1/2 & 0 \\ 0 & 0 & 3 \end{pmatrix} \tag{2a}$$

and

$$\boldsymbol{P}^{-1} = \boldsymbol{Q} = \begin{pmatrix} 1/2 & -1/2 & 0 \\ 0 & 2 & 0 \\ 0 & 0 & 1/3 \end{pmatrix}. \tag{2b}$$

The obtained values are $\boldsymbol{a}' = 2\boldsymbol{a}$, $\boldsymbol{b}' = (\boldsymbol{a}+\boldsymbol{b})/2$, $\boldsymbol{c}' = 3\boldsymbol{c}$ and $x' = (x-y)/2$, $y' = 2y$, $z' = z/3$.The $3 \times \boldsymbol{c}$ cell enlargement has as a consequence that there is a symmetry reduction and a twofold splitting of the atomic positions. This increases the number of free parameters by a factor of three. The two new

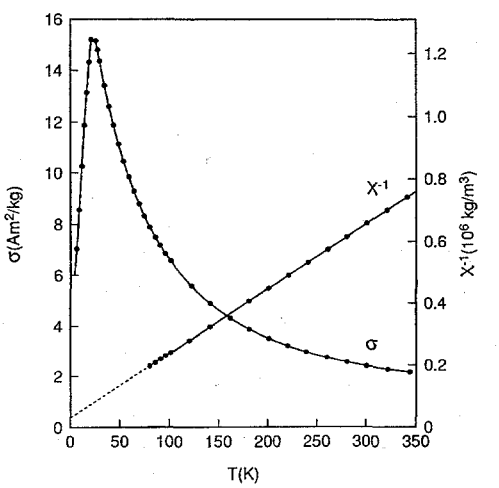

Fig. 1. Temperature dependence of the magnetization σ (left scale) and temperature dependence of the reciprocal susceptibility (χ^{-1}, right scale) of $DyGe_3$. The data were obtained in a field of 1600 kA/m.

atomic positions are 4(c): (0, $-y$, 1/4) and 8(f): $(0,y,z)$ $z = 1/12$ when referring to the orthorhombic cell Cmcm ($\boldsymbol{a},\boldsymbol{b},3\boldsymbol{c}$), which is a maximal isomorphic subgroup of lowest index (order 3) of the space group Cmcm ($\boldsymbol{a},\boldsymbol{b},\boldsymbol{c}$) [3]. The corresponding monoclinic parameters of the two positions are 4e: $(x',y',1/4)$ and 8f: (x',y',z'), $z' = 1/12$. Their numerical values are summarized in Table 1.

3.2. The magnetic structure

The magnetic modes allowed for the Dy(1) atoms at the 8f symmetry site in the magnetic space group $Pa2_1/m$, are given in Table 2. This position may have a general magnetic moment direction while Dy(2) which is situated at the mirror plane m_z can only have a m_z component. The observed A_zA_{-z}

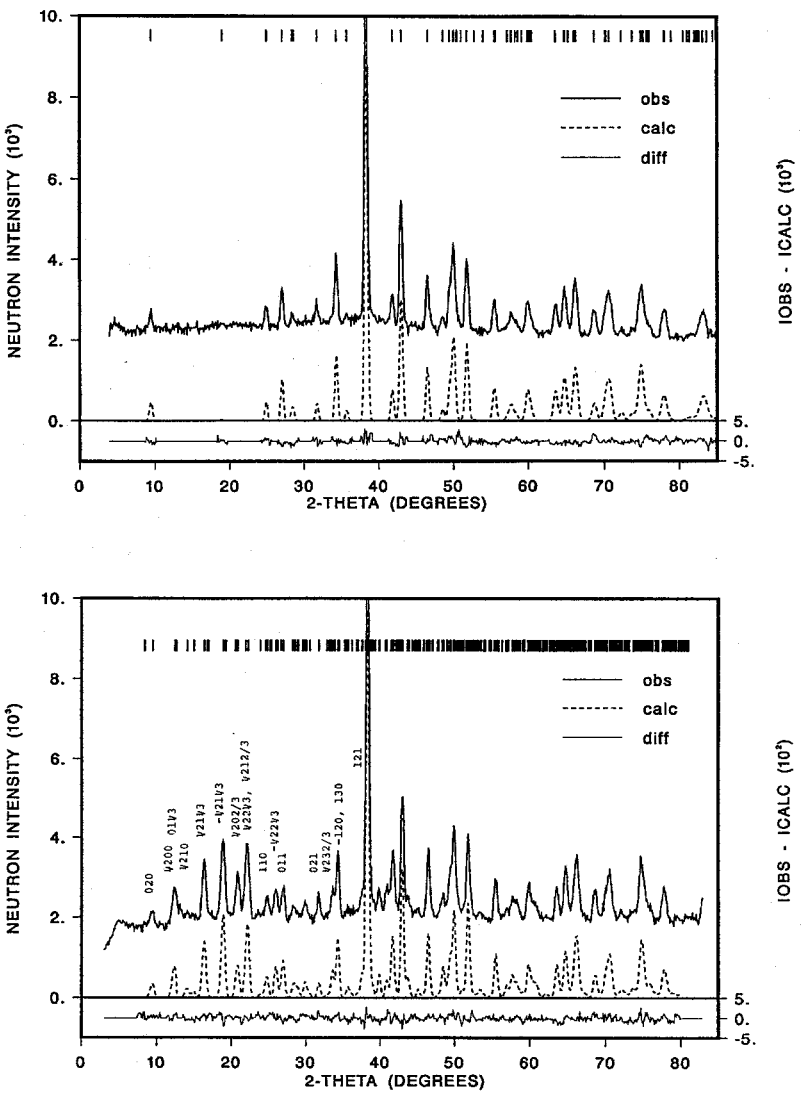

Fig. 2. Observed (solid line) and calculated (broken line) neutron diffraction pattern ($\lambda = 1.7012$ Å) of the compound $DyGe_3$ in the paramagnetic state at 30 K (top), and the magnetically ordered state at 8 K (bottom).

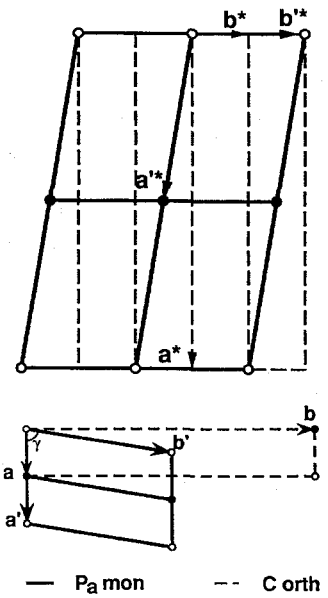

Fig. 3. Base centered orthorhombic C-cell (a,b,c) in direct space (bottom), and in reciprocal space (a^*,b^*,c^*) (top) when viewed along [001]. Solid lines denote the cell of the P_a magnetic lattice and the corresponding (a'^*,b'^*,c'^*) cell.

$(+--+\ \ -++-)$ mode is compatible with the magnetic space group P_a2_1/m when an origin shift of (1/4, 0, 0) has been taken into account.

The refinement has shown that both Dy sites have a collinear arrangement with the magnetic moments confined to the c direction but coupled antiferromagnetically. The moments of the same sublattice have the same sign within the lower half of the monoclinic magnetic cell ($1/2a'$,b',c') and change sign when going from cell to cell in the a direction

Table 2
Symmetry transformations and magnetic modes for the 8f site in the magnetic space group P_a2_1/m with origin shift (1/4, 0, 0)

x	y	z	C_xC_{-x}	C_yC_{-y}	A_zA_{-z}
x	y	z	+	+	+
$-x$	$-y$	$1/2+z$	+	+	−
$-x$	$-y$	$-z$	−	−	−
x	$-y$	$1/2-z$	−	−	+
$1/2+x$	y	z	−	−	−
$1/2-x$	$-y$	$1/2-z$	−	−	+
$1/2-x$	$-y$	$-z$	+	+	+
$1/2+x$	$-y$	$1/2-z$	+	+	−

because of the (1/2, 0, 0) anti-translation (see Fig. 4). The refined ordered moment values of the two Dy positions are equal ($8.1\mu_B$) within experimental error (see Table 3). These values fall below the free-ion value ($gJ\mu_B = 10\mu_B$ for Dy^{3+}), presumably due to crystal field effects.

If one neglects the position parameter deviations from the ideal values of the two Dy positions their change in sign along the c direction can be described as a collinear antiphase domain stacking of the type $\pm(+--)$ of translationally equivalent atoms with different moment values, which results in the $3\times c$ cell enlargement as shown in Fig. 4.

An alternative description of this structure can be given in the form of a modulated magnetic structure of the basic monoclinic cell a, $(a+b)/2$, c which contains the two magnetic atoms Dy(1) at $r_1 =$ (0.576, 0.836, 1/4) and Dy(2) at $r_2 = (0.424, 0.164, 3/4) = -r_1$, and the two observed wave vectors, $k_1 = (1/2, 0, 0)$ and $k_2 = (1/2, 0, 1/3)$. In terms of

Table 1
Atomic parameters of $DyGe_3$. The orthorhombic Cmcm cell: odd atoms occupy the 8f $(0,y,z)$ and even atoms the 4c $(0,y,1/4)$ sites. Magnetic monoclinic cell with space group P_a2_1/m (Sh_{11}^{56}): odd atoms occupy the 8f (x',y',z') and even atoms the 4e $(x',y',1/4)$ sites.

Atom	Orthorhombic (a, b, $3c$)		Monoclinic [$2a$, $(a+b)/2$, $3c$])		
	y	z	x'	y'	z'
Dy(1)	0.4179	1/12	0.7910	0.8358	1/12
Dy(2)	0.5821	1/4	0.7089	0.1642	1/4
Ge(1)	0.0380	1/12	0.9810	0.0760	1/12
Ge(2)	0.9620	1/4	0.5190	0.9240	1/4
Ge(3)	0.6916	1/12	0.6542	0.3832	1/12
Ge(4)	0.3084	1/4	0.8458	0.6168	1/4
Ge(5)	0.8095	1/12	0.5952	0.6190	1/12
Ge(6)	0.1905	1/4	0.9047	0.3810	1/4

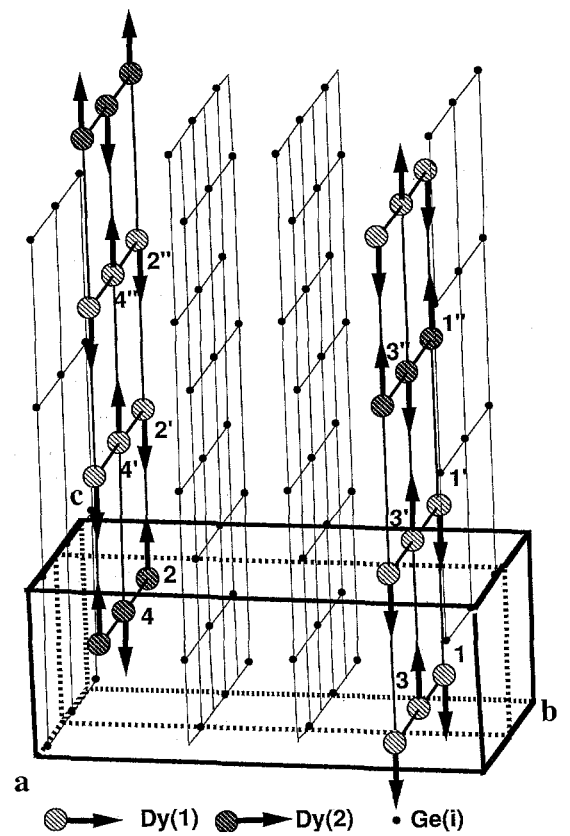

Fig. 4. The low-temperature collinear magnetic structure with the Dy(1) and Dy(2) sublattices coupled antiferromagnetically in $DyGe_3$.

a Fourier representation [5–7] any periodic magnetic moment arrangement with the moments at positions $\boldsymbol{R}_{n\nu} = \boldsymbol{r}_\nu + \boldsymbol{R}_n$, where $\boldsymbol{R}_n = n_1\boldsymbol{a} + n_2\boldsymbol{b} + n_3\boldsymbol{c}$ (n_i = integer and $\nu = 1,2$) can be expressed by the formula

$$\boldsymbol{M}_\nu(\boldsymbol{R}_n) = \sum_j \boldsymbol{Q}_\nu(\boldsymbol{k}_j)\exp(\mathrm{i}\boldsymbol{k}_j \cdot \boldsymbol{R}_{n\nu})$$

$$= \sum_j \boldsymbol{Q}_\nu(\boldsymbol{k}_j)\cos(\boldsymbol{k}_j \cdot \boldsymbol{R}_n + \varphi_{j\nu}), \qquad (3)$$

where $\boldsymbol{k}_j$ are the propagation vectors. Here we would like to note that, because of the anti-translation (1/2, 0, 0), one observes only two sets of magnetic satellite reflections ($\boldsymbol{H} \pm \boldsymbol{k}_j$) pertaining to the wave vectors $\boldsymbol{k}_1$ and $\boldsymbol{k}_2$. Because the moments are along $\boldsymbol{c}$, the vectors $\boldsymbol{Q}_\nu(\boldsymbol{k}_j)$ are also along $\boldsymbol{c}$. The 12 moments in the enlarged magnetic unit cell: $\boldsymbol{M}_0$, $\boldsymbol{M}_1$, $\boldsymbol{M}_2$ for the atoms $\boldsymbol{r}_\nu$, $\boldsymbol{r}_\nu + \boldsymbol{c}$, $\boldsymbol{r}_\nu + 2\boldsymbol{c}$, and $-\boldsymbol{M}_0$, $-\boldsymbol{M}_1$, $-\boldsymbol{M}_2$ for those at $\boldsymbol{r}_\nu + \boldsymbol{a}$, $\boldsymbol{r}_\nu + \boldsymbol{ac}$, $\boldsymbol{r}_\nu + \boldsymbol{a} + 2\boldsymbol{c}$ for $\nu = 1$, and $\pm\boldsymbol{M}_i$ for $\nu = 2$. The moment arrangement along the chains $\boldsymbol{r}_{n2}$ and $\boldsymbol{r}_{n3}$ corresponds to a shift by $2/3\boldsymbol{c}$ to that of chains $\boldsymbol{r}_{n1}$ and $\boldsymbol{r}_{n4}$. Then the vectors $\boldsymbol{Q}_\nu(\boldsymbol{kj})$ can be found by rewriting formula (3) for $\boldsymbol{M}_\nu(\boldsymbol{r}_n)$ as

$$\boldsymbol{M}_\nu(\boldsymbol{R}_n) = \boldsymbol{Q}_1^\nu \cos(\boldsymbol{k}_1 \cdot \boldsymbol{R}_n) + \boldsymbol{Q}_2^\nu \cos(\boldsymbol{k}_2 \cdot \boldsymbol{R}_n)$$

$$+ \boldsymbol{Q}_3^\nu \sin(\boldsymbol{k}_2 \cdot \boldsymbol{R}_n), \qquad (4)$$

Table 3
Refined parameters from the 8 K neutron diffraction data (magnetically ordered state) of $DyGe_3$. Magnetic space group P_a2_1/m (enlarged cell [$2\boldsymbol{a}$, ($\boldsymbol{a} + \boldsymbol{b}/2$, $3\boldsymbol{c}$)]

Atom	Parameters at 8 K			
	x	y	z	μ_z (μ_B)
Dy(1)	0.785(1)	0.831(1)	0.083	8.2(5)
Dy(2)	0.712(2)	0.158(2)	0.25	−8.1(5)
Ge(1)	0.983(8)	0.079(4)	0.083	
Ge(2)	0.509(11)	0.916(9)	0.25	
Ge(3)	0.627(5)	0.388(3)	0.083	
Ge(4)	0.857(15)	0.621(6)	0.25	
Ge(5)	0.935(7)	0.368(5)	0.25	
Ge(5)	0.593(6)	0.615(3)	0.083	
Ge(6)	0.935(7)	0.368(5)	0.25	
$B_{0\nu}$ (nm^2)	0.013(1)			
a, b, c (nm), γ (deg)	0.80584(12)	1.05484(19)	1.16902(17)	79.047(17)
R_n, R_m, R_{wp} (%)	5.15, 10.14, 13.40	R_{exp} (%), χ^2	7.75, 2.49	

with

$$Q_1^\nu = \frac{M_0 + M_1 + M_2}{3}, \qquad Q_2^\nu = \frac{2M_0 - M_1 - M_2}{3},$$

$$Q_3^\nu = \frac{M_1 - M_2}{\sqrt{3}}, \tag{5}$$

for $\nu = 1$ and, analogously, with M_i' for $\nu = 2$. In (3) $\varphi_{1\nu}$ can be put equal to zero and therefore the index j can be suppressed, $\varphi_{2\nu} = \varphi_\nu$. Consequently,

$$\tan \varphi_\nu = -Q_3^\nu / Q_2^\nu, \qquad Q_\nu(k_1) = Q_1^\nu,$$

$$Q_\nu(k_2) \cos \varphi_\nu = Q_2^\nu. \tag{6}$$

If there is a symmetry relation between $\nu = 1$ and $\nu = 2$ there are not six but three parameters. Moreover, one may put in a result from Landau theory that states that $\varphi_{j\nu}$ is restricted, and for a special choice of origin can be put equal to 0 or $\pi/3$.

The moment arrangement $M_0 = -M_1 = -M_2$ (Fig. 4) found from the refinement at temperatures $T < 10$ K, corresponds to $Q_1^\nu = M_0/3 = M/3$, $Q_2^\nu = 4M/3$ and $Q_3^\nu = 0$ and $\varphi_\nu = 0$ for the chain r_{n1} with origin at atom 1″. As will be shown below, the ratio $Q_1^\nu / \{Q_2^{\nu\,2} + Q_3^{\nu\,2}\}^{1/2}$ is temperature dependent.

3.3. The temperature dependence of the magnetic intensities

Given the fact that in several members of the R–Ge family, including $TbGe_3$, phase transitions comprising incommensurate phases were frequently observed, five neutron patterns were collected in the region 8–25 K. From these data it turns out that the positions of the magnetic reflections remain unchanged up to T_N and therefore the wave vectors k_1 and k_2 remain commensurate with the crystal lattice. On the other hand, one observes a rapid intensity decrease of the unique observed reflection (1/2, 0, 0) ($2\theta = 12.3°$) associated with the Fourier coefficients $Q_\nu(k_1)$, as shown in the refined neutron pattern at 14 K (see Fig. 5) compared with those of $Q_\nu(k_2)$. This indicates a change in the ratio $Q_1^\nu / \{Q_2^{\nu\,2} + Q_3^{\nu\,2}\}^{1/2}$ as a function of temperature. In terms of Eqs. (4)–(6) it finally results in the different temperature-dependent behaviours of the moments of the two Dy positions, as given in Table 2 (for the enlarged magnetic cell).

In fact, contrary to the results obtained at 8 K, the refined moment values of the two Dy positions are

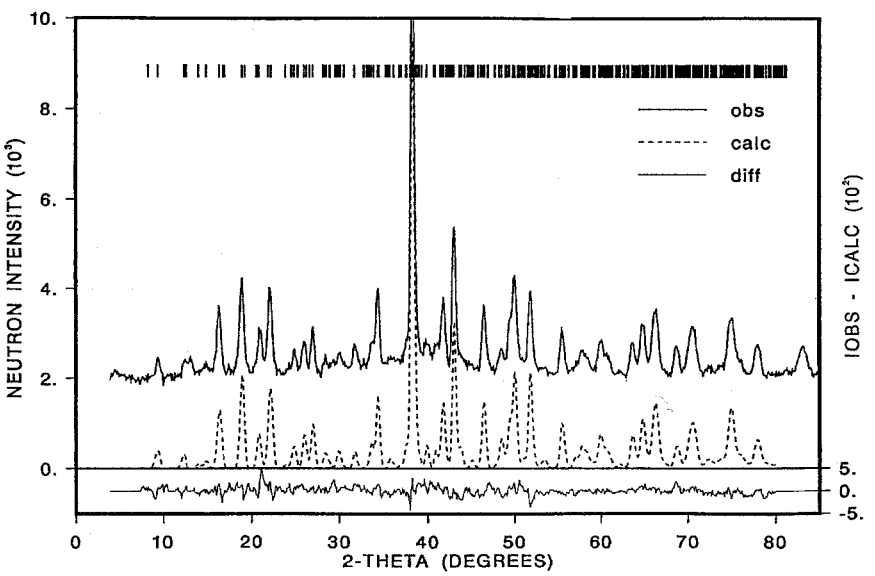

Fig. 5. Observed (solid line) and calculated (broken line) neutron diffraction pattern of the compound $DyGe_3$ in the magnetically ordered state at 14 K.

different at 14 K. The corresponding values are $6.8(7)\mu_B$ and $8.6(6)\mu_B$ for Dy(1) and Dy(2), respectively. Although these values have a larger error than for the 8 K data, this result is supported by the strong change in the intensity of the (1/2, 0, 0) reflection. The contributions of the two Dy positions to the structure factor expression of this reflection have opposite signs $4 \times 0.97i(2\mu_{Dy(1)} - \mu_{Dy(2)}) \approx \boldsymbol{Q}_\nu(\boldsymbol{k}_1)$, which change abruptly when $\mu_{Dy(1)}$ becomes smaller than $\mu_{Dy(2)}$.

To derive the temperature dependence of the two sublattices we have measured the temperature dependencies of the intensities of two representative reflections $(1/2, 0, 0) \approx \boldsymbol{Q}_\nu(\boldsymbol{k}_1)^2$ and $(1/2, 1, 1/3) \approx \boldsymbol{Q}_\nu(\boldsymbol{k}_2)^2$, which in fact display quite different behaviours with T. These temperature dependencies are shown in Fig. 6. The upper curve represents the intensity of the reflection (1/2, 1, 1/3) where the contributions of the two Dy sublattices add in the structure factor. The different behaviour compared to the (1/2, 0, 0) reflection indicates a change in the relative moment values. The temperature dependencies of these two reflections have been used to derive the temperature dependencies of the moments of the two Dy sites shown at the top of Fig. 7. One may distinguish three different regions with the temperature. Both sites start to order at $T_N = 24$ K, the moments μ_2 are seen to increase quite abruptly and to reach saturation already at $T_1 = 19$ K, while the increase in the moments μ_1 occurs much more smoothly and reaches saturation below $T_2 = 10$ K. One may realize that in the temperature range I (19 K $< T <$ T_N) the moment ratio remains constant and approximates $\mu_1/\mu_2 = 1/2$, while in range II (10 K $< T <$ 19 K) this ratio changes continuously to reach the value 1 for $T < 10$ K. One also gets the impression that the moment value of Dy(2) decreases slightly below 19 K.

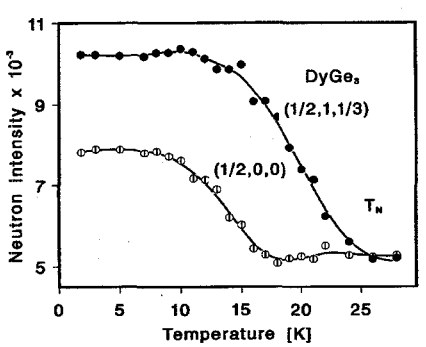

Fig. 6. Temperature dependence of the magnetic intensity of the reflections (1/2, 0, 0) and (1/2, 0, 1/3) of $DyGe_3$ associated with the Fourier components $\boldsymbol{Q}_1^\nu$ and $\boldsymbol{Q}_2^\nu$ (different structure factor contributions).

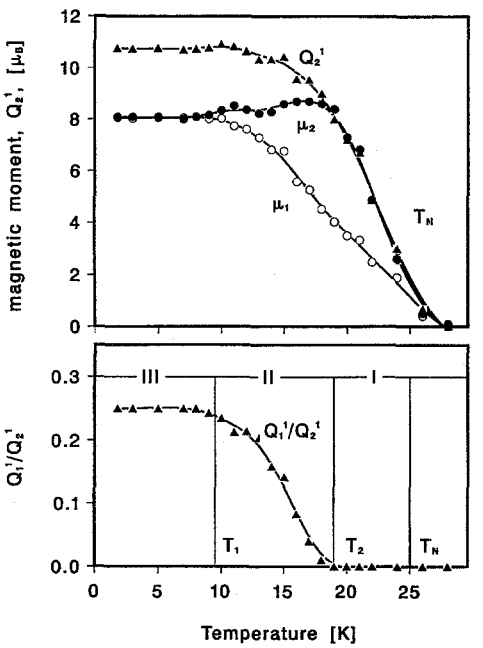

Fig. 7. Temperature dependence of (top) the moments μ_1 and μ_2 of the two Dy positions as derived from the data shown in Fig. 6 ($\mu_1 = M_1 = M_2$ and $\mu_2 = M_0$, cf. Eq. (5)); and (bottom) the Fourier components $\boldsymbol{Q}_2^1$ (amplitude of Dy atom 1″ in Fig. 4) and (bottom part) of the ratio $\boldsymbol{Q}_1^1/\boldsymbol{Q}_2^1$.

3.4. The squaring up of the modulated structure

This rather unusual temperature behaviour of the magnetic moments can be explained more adequately for the structure description given in Section 2.2 in terms of three Fourier coefficients $\boldsymbol{Q}_1^\nu$ over the whole temperature range. As already mentioned, when choosing the origin at the atom 1″ one finds $\varphi_1 = 0$ and $\boldsymbol{Q}_3^\nu = 0$ for that atom, and therefore $\boldsymbol{M}_1 = \boldsymbol{M}_2$ in (5) over the whole temperature range. One may then calculate $\boldsymbol{Q}_1^1$ and $\boldsymbol{Q}_2^1$ from Eq. (5) and the refined moment values shown in Fig. 6, where $\mu_2 = \boldsymbol{M}_0$ and $\mu_1 = \boldsymbol{M}_1 = \boldsymbol{M}_2$. The behaviour of $\boldsymbol{Q}_2^1$ is included in the top part of Fig. 7, and the ratio of $\boldsymbol{Q}_1^1/\boldsymbol{Q}_2^1$ is shown in the bottom part. On the basis of

Fig. 7 (bottom part) one may distinguish the three regions of different behaviour in the following way.

In the high-temperature region I (19 K $< T_N$) $Q_1^1 = 0$, and therefore the ratio Q_1^1/Q_2^1 is also zero. In this region the moments along the c chain maintain the same orientation but their relative values are described by only one harmonic function with the Fourier coefficients Q_2^1, and therefore $M_0/2 = -M_1 = -M_2$. In this region the structure is purely a longitudinally sine wave modulated structure with amplitude M_0 or an antiphase domain structure with two different amplitudes ($M_0/2 = -M$).

In the intermediate region (II) the Q_1^1/Q_2^1 ratio increases from 0 to 1/4 with decreasing temperature, and the collinear modulated structure begins to square up. In this region two different amplitudes (M_0 and M) are necessary for its description.

In the low-temperature region III ($T < 10$ K) the ratio $Q_1^1/Q_2^1 = 1/4$, and all the atoms have the same amplitude but different signs $M_0 = M_1 = -M_2 = -M$, so that the arrangement along the c direction is 'ferrimagnetic' (antiphase domain $++-++-\cdots$).

4. Concluding remarks

The occurrence of a sine wave or antiphase domain (with two amplitudes) high-temperature magnetic phase between T_1 and T_N which at a lower temperatures ($T < T_1$) undergoes transition a progressive squaring up to a collinear antiphase domain structure with equal moment without any change in the wave vector length $k_2 = (1/2, 0, 1/3)$ is also found for the isomorphic $TbGe_3$ [8]. For the latter compound however, the magnetic lattice requires a sixfold cell enlargement of the orthorhombic C cell ($2a,b,3c$) because the atoms related by the C-centering operation have opposite moments. Both compounds have their main axis of antiferromagnetism along c, parallel to the direction of linear chains with the smallest distance, as observed for the parent DyGe and the high-temperature modification of the TbGe compound [2].

The squaring up of the magnetically modulated high-temperature structure manifests itself by the onset of the magnetic satellites associated with a second wave vector $k_1 = (1/2, 0, 0)$ observable in the neutron pattern at lower temperatures. The ratio of the observed Fourier coefficients Q_1^1/Q_2^1 pertaining to the two vectors is a measure of the degree of the continuous transition from the sinusoidal to the antiphase domain type. The temperatures T_1 and T_2 shown in Fig. 7 do not in fact represent real transition temperatures because no discontinuities in either the Dy moment value or the wave vectors have been observed. The existence of uniaxial magnetic moment arrangements indicates the existence of a strong crystal field anisotropy, and the presence of two wave vectors indicates the presence of competing interactions leading to complex ordering mechanisms.

A similar squaring up mechanism that can be described with the help of two wave vectors $q_1 = 1/3b^*$, $q_2 = 0$ has been reported for the orthorhombic $DyGe_2$ and $TbCu_2$ compounds [9,10]. These compounds also display high-temperature collinear modulated magnetic structures, and calculations of the exchange energies [11,12] have shown that the description of the complex transition mechanisms occurring in both the $DyGe_2$ and $TbCu_2$ compounds requires a 12-sublattice model with Ising spin $S = 1/2$ and the assumption of four kinds of exchange interactions. Most likely a similar mechanism is operative in the $DyGe_3$ and $TbGe_3$ compounds.

References

[1] P. Schobinger-Papamantellos, D.B. de Mooij and K.H.J. Buschow, J. Alloys and Compounds 183 (1992) 181.
[2] K.H.J. Buschow, P. Schobinger-Papamantellos and P. Fischer, J. Less-Common Metals 139 (1988) 221.
[3] Th. Hahn, ed., International Tables for Crystallography, vol. A (Reidel, Dordrecht, 1983).
[4] V.A. Koptsik, Shubnikov Groups (Moscow University, 1966).
[5] D.H. Lyons, T.A. Kaplan, K. Dwight and N. Menyuk, Phys. Rev. 126 (1962) 540.
[6] P. Fischer, G. Meier, W. Hälg, B. Lebech, B.D. Rainford and O. Vogt, Risö Report No. 369 (1977).
[7] P. Fischer, B. Lebech, G. Meier, B.D. Rainford and O. Vogt, J. Phys C: Solid State Phys. 11 (1978) 345.
[8] P. Schobinger-Papamantellos, J. Rodríguez-Carvajal, T. Janssen and K.H.J. Buschow, Int. Conf. Aperiodic '94, Les Diablerets, Switzerland, 18–22 Sept. 1994.
[9] B. Lebech, Z. Smetana and V. Sima, J. Magn. Magn. Mater. 70 (1987) 97.
[10] V. Sima, Z. Smetana, B. Lebech and E. Gratz, J. Magn. Magn. Mater. 54 (1986) 1357.
[11] I. Kimura, J. Magn. Magn. Mater. 52 (1985) 199.
[12] I. Kimura, J. Magn. Magn. Mater. 70 (1988) 273.